Chemosphere 92 (2013) 368–374

Contents lists available at SciVerse ScienceDirect

Chemosphere

journal homepage: www.elsevier.com/locate/chemosphere

Enhanced reduction of chlorophenols by nanoscale zerovalent iron supported on organobentonite

Yimin Li [a,*], Yun Zhang [a,b], Jianfa Li [a], Guodong Sheng [a], Xuming Zheng [b]

[a] College of Chemistry and Chemical Engineering, Shaoxing University, Zhejiang 312000, PR China
[b] Department of Chemistry and State Key Laboratory of ATMMT (MOE), Zhejiang Sci-Tech University, Hangzhou 310018, PR China

HIGHLIGHTS

- CMTA-Bent enriched chlorophenol(CP)s on NZVI surface and enhanced the reduction.
- The enhancement on reduction rate is positively related to CPs' hydrophobicity.
- NZVI/CTMA-Bent showed good reusability due to fewer precipitates on iron surface.

GRAPHICAL ABSTRACT

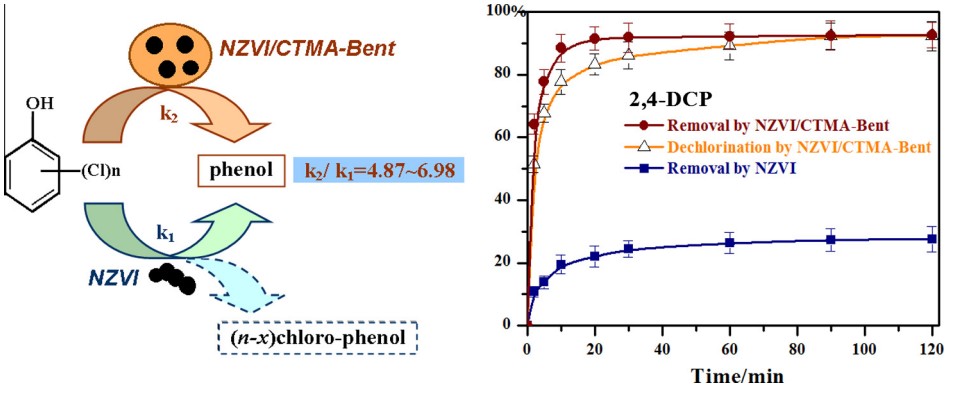

ARTICLE INFO

Article history:
Received 6 September 2012
Received in revised form 13 December 2012
Accepted 7 January 2013
Available online 8 February 2013

Keywords:
Organobentonite
Nanoscale zerovalent iron
Chlorophenols
Reduction
Synergetic effect

ABSTRACT

The reactivity of nanoscale zerovalent iron (NZVI) on removing chlorophenols (2-chlorophenol, 2,4-dichlorophenol, 2,4,6-trichlorophenol and pentachlorophenol) was remarkably enhanced by using a hydrophobic support of organobentonite (CTMA-Bent), namely the bentonite modified with organic cetyltrimethylammonium (CTMA) cations. The complete dechlorination of chlorophenols and total conversion into phenol using this novel NZVI/CTMA-Bent combination was observed in batch experiments. The kinetic studies suggested that the reduction of chlorophenols by NZVI was accelerated due to the enhanced adsorption onto CTMA-Bent, which facilitated the mass transfer of chlorophenols from aqueous to iron surface. The enhanced reduction rate by NZVI/CTMA-Bent was positively related to the hydrophobicity of chlorophenols, and an increasing linear relationship was obtained between the relative enhancement on reaction rate constants (k_2/k_1) and $\log K_{ow}$ values of chlorophenols. XPS results suggested there were fewer precipitates of ferric (hydro)xides formed on the surface of NZVI/CTMA-Bent, which may also lead to the improved reactivity and repetitive usability of NZVI/CTMA-Bent on removing chlorophenols.

1. Introduction

Zerovalent iron (ZVI) has been suggested as a promising candidate for the removal of a wide range of organic contaminants (Gillham and O'Hannesin, 1994; Cao et al., 1999; Dries et al., 2004; Yoon et al., 2011; Habekost and Aristov, 2012). However, its reaction rate with chlorinated aromatics is slow, with half-lives of days or longer calculated by a pseudo-first-order kinetics (Sayles et al., 1997; Feng and Lim, 2005). The slow reduction may result in the accumulation of toxic byproducts from partial dechlorination (Liu et al., 2005), and introduce new contaminants in the environment. As the reduction of contaminants by ZVI is surface mediated, the reaction rate is positively related to the concentration of

* Corresponding author. Address: College of Chemistry and Chemical Engineering, Shaoxing University, Huancheng West Road 508, Shaoxing, Zhejiang 312000, China. Tel.: +86 575 8834 2386; fax: +86 575 8831 9253.
E-mail address: liym@usx.edu.cn (Y. Li).

0045-6535/$ - see front matter © 2013 Elsevier Ltd. All rights reserved.
http://dx.doi.org/10.1016/j.chemosphere.2013.01.030

contaminants around the iron surface (Loraine, 2001; Wu and Ritchie, 2006), which could be increased by improving hydrophobicity of iron surface. For example, modification of ZVI with cationic surfactants enhanced the reduction rate for perchloroethylene (PCE) by an order of magnitude (Alessi and Li, 2001). In such a system, the sorbed cationic surfactants on ZVI served as hydrophobic mosaics for PCE partitioning, and increased PCE concentration on reactive sites of iron and thus enhanced the reduction rate. Combining surfactant-modified zeolite (SMZ) with ZVI in a palletized form also showed dramatic enhancement on PCE removal (Li et al., 1999). It was speculated that concentration of chlorinated contaminants in the vicinity of iron surface was increased by the sorption of SMZ, and then the mass transfer was enhanced (Zhang et al., 2002; Cho and Park, 2006).

Nanoscale zerovalent iron (NZVI) with larger specific surface area is another choice for enhancing the reactivity of iron on removing contaminants (Wang and Zhang, 1997). The reduction rate of chlorinated organics was dramatically enhanced, and fewer chlorinated byproducts were observed using nanoscale iron particles (Wei et al., 2006; Cho and Choi, 2010). In addition, NZVI particles have potential for in situ remediation (Choe et al., 2001; Elliott and Zhang, 2001), because they may be directly injected as a slurry into contaminated subsurface zones. However, NZVI particles exhibit strong tendency to agglomerate into larger ones due to the high surface energy and intrinsic magnetic interaction. This results in adverse effect on both effective surface area and removal performance (Zheng et al., 2008). Besides, the separation and recycling of bare nanoscale particles from aqueous phase is extremely difficult (Wang et al., 2008a,b). To overcome these drawbacks, several solid have been developed serving as supporting materials of NZVI (Ponder et al., 2000). For example, cellulose derivatives (Wu and Ritchie, 2006; Cho and Choi, 2010) and silica (Zheng et al., 2008; Saad et al., 2010) could help to inhibit the aggregation of NZVI particles. Cation exchange resin, as the carrier of NZVI, promoted the removal efficiency to decabrominated diphenyl ether and water-soluble azo dyes (Li et al., 2007). However, some of these immobilization methods are complex, while some supporting materials are not hydrophobic enough, and they did not perform well on enriching organic contaminants due to their limited adsorption to organic compounds.

Modified bentonites, as good sorbents prepared from cheap bentonite by simple cation exchange reactions, have been investigated on the removal of various contaminants in the past decades (Zhu et al., 1997; Ma and Zhu, 2007). Both inorganic and organic cations containing various functional groups have been used in the bentonite modifications, and the dose of cations for exchange reaction is adjustable. Therefore, the structure and properties (e.g. hydrophobicity) of modified bentonites can be designed to achieve high adsorption to target contaminants. When the modified bentonites are used together with ZVI, its reactivity with target contaminants will be enhanced because of the enrichment of contaminants to the solid iron surface (Cho et al., 2005; Li et al., 2010).

The objective of this work is to enhance the reactivity of NZVI to chlorinated aromatics by using a support of organobentonite (CTMA-Bent), a modified bentonite prepared by cation exchange reaction with organic cetyltrimethylammonium cations. The organic phase in this support will improve the hydrophobicity of iron surface and have organic contaminants enriched around the reactive sites, so an enhanced reactivity on removing contaminants is expected. For this purpose, a series of chlorophenols (CPs) were employed as the target contaminants, including 2-chlorophenol (2-CP), 2,4-dichlorophenol (2,4-DCP), 2,4,6-trichlorophenol (2,4,6-TCP) and pentachlorophenol (PCP). The reaction kinetics of CPs with NZVI/CTMA-Bent will be investigated by Langmuir–Hinshelwood (L–H) model, and compared with that by NZVI, so as to discuss the role of CTMA-Bent in the combined reduction system. Furthermore, X-ray photoelectron spectroscopy (XPS) is employed for surface element investigation to determine the distribution and valence state of iron on the surface of NZVI or NZVI/CTMA-Bent samples.

2. Materials and methods

2.1. Materials

The original bentonite composed primarily of Na^+-montmorillonite (Na-Bent) was purchased from Inner Mongolia, China. Its cation exchange capacity (CEC) is 115 cmol kg^{-1}. Commercial iron powder (100 mesh, Fe^0) and other chemicals of analytical grade were purchased from Shanghai Chemical Co., China: ferrous sulfate heptahydrate ($FeSO_4{\cdot}7H_2O$), sodium borohydride ($NaBH_4$), cetyltrimethylammonium bromide (CTMA), sodium hydroxide (NaOH), 2-CP (C_6H_5ClO), 2,4-DCP ($C_6H_4Cl_2O$), 2,4,6-TCP ($C_6H_3Cl_3O$) and PCP (C_6HCl_5O).

2.2. Synthesis and characterization of organobentonite and NZVI samples

The organobentonite was prepared by a cation exchange process (Li et al., 2008). CTMA was added to a 1% (w/w) aqueous suspension of 20.0 g of Na-Bent under continuous stirring for 120 min in a water bath at 70 °C. The molar amount of CTMA added was equal to the CEC of Na-Bent, and then, the suspension was centrifuged, washed and dried to a constant weight. Finally, the solid was mechanically ground to less than 0.15 mm in size and heated at 115 °C for 120 min before use. The final product was denoted as CTMA-Bent.

NZVI particles were obtained through reduction of $FeSO_4{\cdot}7H_2O$ by dropwise addition of an excessive amount of $NaBH_4$ under stirring (Phenrat et al., 2007). The reaction could be represented as

$$Fe(H_2O)_6^{2+} + 2BH_4^- \rightarrow Fe^0 \downarrow + 2B(OH)_3 + 7H_2 \uparrow \quad (1)$$

The solution was stirred for another 30 min under room temperature. The metal particles formed were settled and filtered. Then the solid was washed with ethanol for several times, and finally vacuum-dried. The preparation was operated under a nitrogen atmosphere. The final product was labeled as NZVI. The immobilized NZVI was prepared by a similar procedure as described above, except that CTMA-Bent was soaking in $FeSO_4{\cdot}7H_2O$ solution under continuous stirring overnight before the addition of $NaBH_4$ solution (Li et al., 2011). The final product was labeled as NZVI/CTMA-Bent.

The X-ray diffraction (XRD) measurement of NZVI and NZVI/CTMA-Bent has confirmed the formation of iron in its zerovalent state with its major reflection at $2\theta = 44.8°$. BET specific surface areas were determined to be 33.5 $m^2\,g^{-1}$ for NZVI, and 29.5 $m^2\,g^{-1}$ for NZVI/CTMA-Bent. Their iron contents were measured to be 75.3% and 16.8%, respectively.

2.3. Batch experiments for the removal of CPs

The removal of CPs was conducted in conical flask containing 100 mL of CP solution (pH = 5.5) of 0.500 mM ($[CP]_0$) under stirring. Iron samples including NZVI (0.0797 g) and NZVI/CTMA-Bent (0.357 g) were added respectively in the CP solutions. In these treatments, the two iron samples were used at the same dose of iron of 0.600 g L^{-1}. The CP solutions were deoxygenated by N_2 stream for 10 min before adding iron samples, and kept sealed with a stopper during the reaction. The experiments were carried out by putting the flask in a thermostatic shaker bath at 25 ± 0.1 °C, with a rotation speed of 150 rpm. At given time

intervals, a solution sample of 0.5 mL was withdrawn and filtered through a 0.22 μm membrane. The CP concentrations at time t ($[CP]_t$) were determined. The removal efficiency was calculated as: percentage of CP removed (%) = $([CP]_0 - [CP]_t)/[CP]_0 \times 100\%$. The concentration of chloride ion at time t ($[Cl^-]_t$) was also determined. The dechlorination ratio was calculated as: dechlorination ratio (%) = $[Cl^-]_t/([CP]_0 \times n) \times 100\%$, where n is the amount of substituted chlorine atoms in the phenol ring of a CP molecule. The data of batch experiments were obtained in triplicates.

The kinetic investigations were conducted by changing the initial CP concentrations to be 0.05, 0.10, 0.20 and 0.50 mM, respectively.

The evaluation of the stability and repetitive usability of iron samples was investigated by repetitive experiments as following: 100 mL solution containing 0.1 mM of CP was mixed with NZVI (0.0797 g) or NZVI/CTMA-Bent (0.357 g). After 120 min, 1 mL of solution was withdrawn from the flask for analysis of CP concentration, and then an additional 1 mL of CP solution of appreciate concentration was added. As a result, the CP concentration and pH was adjusted to be the same at the beginning of four cycles.

2.4. Adsorption isotherm

The adsorption isotherms of CPs on CTMA-Bent were determined by batch equilibrium of 4.0 g L^{-1} CTMA-Bent in 25 mL of CP solution with various initial concentrations in flasks with glass caps. The initial pH in the solution was adjusted to 5.5 with a negligible volume of 0.01 M HCl or NaOH. All the flasks were shaken for 2 h in a thermostatic shaker bath at 25 ± 0.1 °C at 150 rpm. After equilibrium, the suspension was centrifuged and filtered, the equilibrium concentration of CP (C_e, mM) was determined. The adsorbed amount (Q_e, mmol g^{-1}) was calculated from the difference between the initial and equilibrium concentrations according to the following equation, $(Q_e) = [(C_0 - C_e) \times V]/m$, where V (L) is the total volume, and m (g) is the mass of adsorbent.

2.5. Analytical methods

Quantitative analysis of CPs and phenol was performed in an HP1100 (Agilent Technologies, Inc.) high performance liquid chromatography system equipped with a UV–VIS detector and a C-8 column (4.6 mm × 250 mm, 5 μm). A mobile phase of methanol–water mixture (70:30, V/V) was employed at a flow rate of 0.80 mL min^{-1}. The analytical wavelength for phenol, 2-CP, 4-CP was 280 nm, and 285 nm for 2,4-DCP and 2,4,6-TCP, and 295 nm for PCP, respectively.

XPS spectra were reported using a Thermo ESCALAB 250 with a monochromatized Al Kα X-ray source ($h\gamma$ = 1486.6 eV) operated at a power of 150 W and a constant pass energy of 20 eV for the analyzer. Surface charging effects were corrected with C1s peak at 284.8 eV as a reference. A Shirley background correction and Gaussian–Lorentzian fitting were used to transform peak areas to total intensities.

The solution pH was measured with pH meter (PHS-2C, China). The chloride ion concentration during the reaction was measured by a chloride ion-selective electrode (pC1-1, China).

3. Results and discussion

3.1. Enhanced removal of CPs by supported NZVI

The time-dependent removal efficiencies of 2-CP, 2,4-DCP, 2,4,6-TCP and PCP by NZVI/CTMA-Bent and NZVI were shown in Fig. 1, respectively. The corresponding dechlorination kinetics by NZVI/CTMA-Bent are also illustrated in Fig. 1. As can be seen, the maximum removal efficiencies by NZVI for 2-CP, 2,4-DCP,

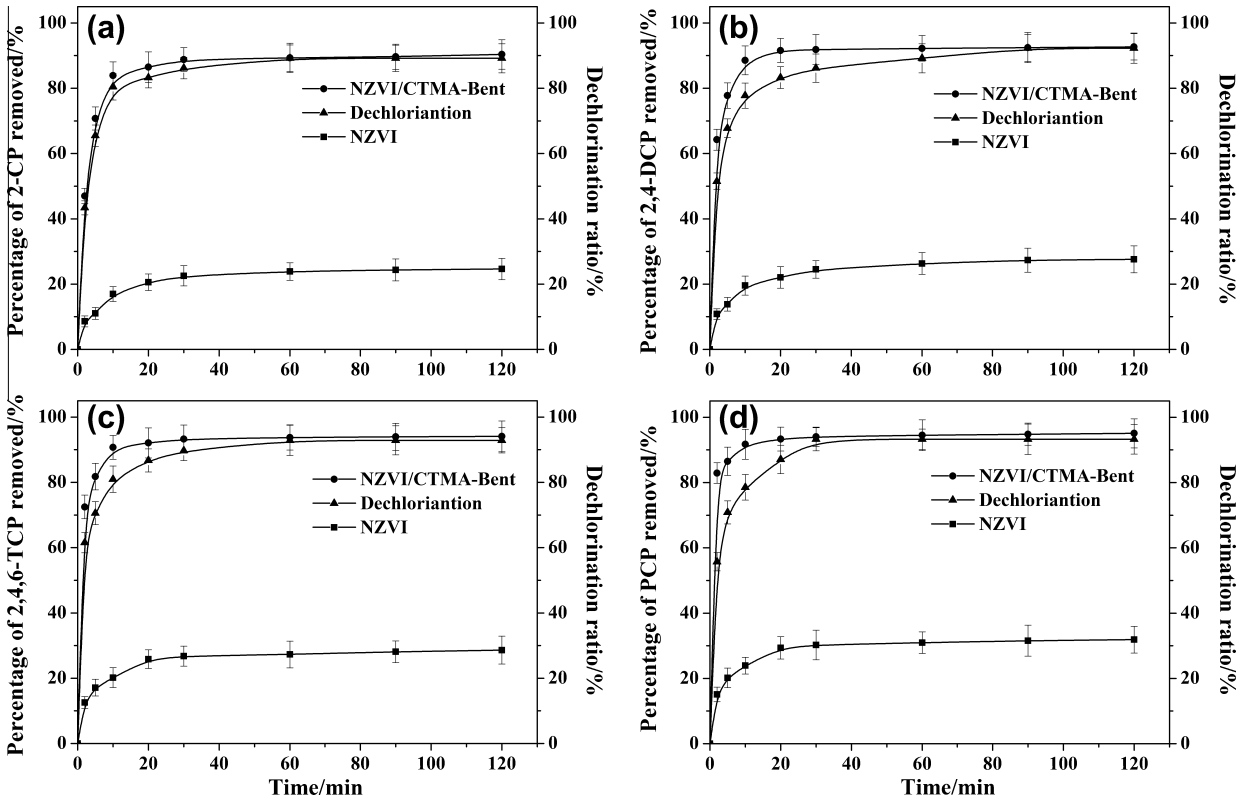

Fig. 1. Removal efficiency and dechlorination rate of 2-CP (a), 2,4-DCP (b), 2,4,6-TCP (c) and PCP (d) by NZVI or NZVI/CTMA-Bent. $[CP]_0$ = 0.50 mM, pH = 5.5, iron dose: 0.60 g L^{-1}.

2,4,6-TCP and PCP were 20.9%, 23.2%, 24.6% and 31.1%, respectively, while the maximum removal efficiencies by NZVI/CTMA-Bent were 88.2%, 91.1%, 92.6% and 94.1%, respectively. Apparently, the removal efficiency of CPs by NZVI/CTMA-Bent was much higher than that by NZVI. The enhanced efficiency may be first related to the morphology of NZVI particles. According to our previous investigation (Li et al., 2011), the bare NZVI sample exists as necklace-like aggregates, whereas NZVI particles immobilized on CTMA-Bent were clearly discrete and well dispersed on the carrier, without aggregation. As a result, the reactive sites of NZVI particles were more accessible for CP molecules, leading to the enhanced removal efficiency. In addition, the removal of CPs by NZVI/CTMA-Bent was accompanied by the release of chloride ions from the phenol ring, by which we could calculate the dechlorination ratios. As is depicted in Fig. 1a–d, the final dechlorination ratios of 2-CP, 2,4-DCP, 2,4,6-TCP and PCP by NZVI/CTMA-Bent were 86.7%, 89.2%, 92.8% and 93.2%, respectively, which are equivalent to the total percentage of corresponding CPs removed (87.1% for 2-CP, 88.9% for 2,4-DCP, 93.1% for 2,4,6-TCP and 93.4% for PCP). This implies that the removal of CPs by NZVI/CTMA-Bent was almost totally attributed to reduction by NZVI instead of adsorption by CTMA-Bent.

For a deeper understanding on the enhanced removal of CPs by NZVI/CTMA-Bent, the chemical conversions of 2,4-DCP after reduction by NZVI and NZVI/CTMA-Bent are shown in Fig. 2. Similar as that reported previously (Kim and Carraway, 2000; Cheng et al., 2010), only partial dechlorination was obtained using NZVI alone. As shown in Fig. 2a, the dechlorination products of 2,4-DCP by NZVI were consisted of 2-CP, 4-CP and phenol, and with some residual 2,4-DCP. In contrast, phenol was the main product of reduction by NZVI/CTMA-Bent. 2-CP and 4-CP were only observed in the initial stage (before 30 min), then, they were converted into phenol (as shown in Fig. 2b). This is in agreement with the dechlorination results discussed above. It demonstrated that, under our experimental condition, 2,4-DCP was almost completely dechlorinated and converted into phenol by NZVI/CTMA-Bent. In view of this, the dechlorination activity of NZVI was significantly enhanced by employing CTMA-Bent as a support. The formation of phenol provided evidence that the enhanced removal of CPs by NZVI/CTMA-Bent was attributed to the synergetic effect between adsorption by CTMA-Bent and reduction by NZVI. In our previous study (Li et al., 2011), the synergetic effect was confirmed by the formation of Cl^- and phenol during the PCP removal process. It was found that both the dechlorination ratio and the summation of phenol in the solid and aqueous phase were in agreement with the percentage of PCP removed in overall. In addition, Li et al. (2011) extracted the PCP in the solid phase using hexane, and no PCP was found. According to these results, it was concluded that the PCP removal by NZVI/CTMA-Bent was dominantly attributed to the reduction by NZVI rather than the adsorption by CTMA-Bent. The adsorption facilitated the mass transfer, and accelerated the removal of PCP in a synergetic way.

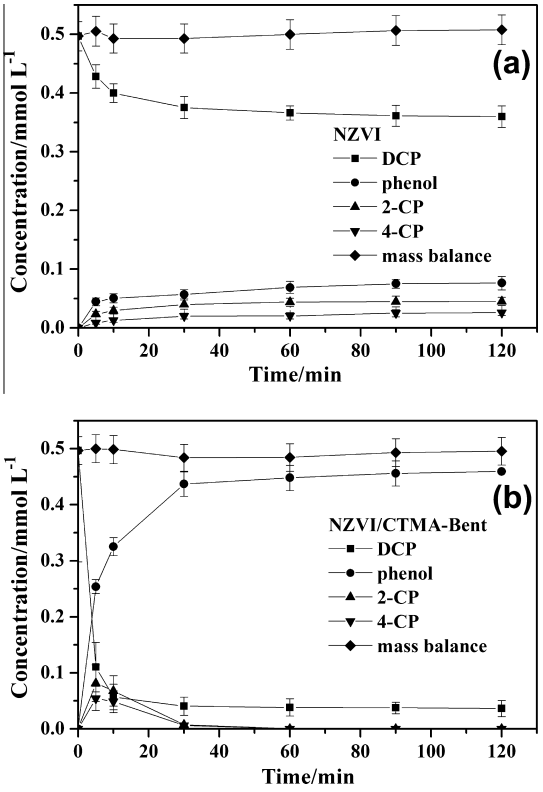

Fig. 2. Chemical conversion of 2,4-DCP during dechlorination by NZVI (a) or NZVI/CTMA-Bent (b).

3.2. Kinetic investigations on the removal of CPs

In order to investigate the role of CTMA-Bent on accelerating the reduction of CPs by NZVI, the removal experiments by NZVI or NZVI/CTMA-Bent were conducted as a function of initial concentration of CPs. The results for removal of 2-CP, 2,4-DCP, 2,4,6-TCP and PCP were shown in Supplementary Material (Fig. SM-1a–d). As can be seen, the enhanced removal by NZVI/CTMA-Bent was observed on each CP at each initial concentration.

The Langmuir–Hinshelwood (L–H) equation (Eq. (2)) was employed to quantitatively describe the surface reaction of CPs on NZVI or NZVI/CTMA-Bent.

$$\frac{1}{r_0} = \frac{1}{kK}\cdot\frac{1}{C_0} + \frac{1}{k} \tag{2}$$

where r_0 is the initial reaction rate, C_0 is the initial concentration of PCP, and k, K are the reaction rate constant and adsorption coefficient, respectively. The initial rate, $r_0 = \Delta c/\Delta t$, was calculated from the decreased concentration (Δc) in the first 2 min (Δt) of reduction.

According to the results in Table 1, we can observe two major tendencies: First, the reaction rate constants of all CPs with NZVI/CTMA-Bent (k_2) were much higher than those with NZVI (k_1), indicating the distinctly accelerated reduction of CPs with the supported system. Second, the reaction rate constants of various CPs with either NZVI (k_1) or NZVI/CTMA-Bent (k_2) can be ranked in the increasing order: 2-CP < 2,4-DCP < 2,4,6-TCP < PCP. This order may be related to the decreasing stability of C–Cl bonds with the increased number of chlorine atoms on the phenol ring. The increasing electron attracting effect by more substituted chlorine atoms leads to the reduced dissociation energy of C–Cl bonds, and makes them more ready to break down (Wang et al., 2008a,b).

Another explanation for the above tendencies may be related to the adsorption of CPs on CTMA-Bent, with adsorption isotherms shown in Supplementary Material (Fig. SM-2). As can be seen,

Table 1
Parameters for Langmuir–Hinshelwood kinetics of CPs removal.

	$\log K_{ow}$	NZVI			NZVI/CTMA-Bent			k_2/k_1
		k_1	K_1	R_1	k_2	K_2	R_2	
2-CP	2.17	0.0862	3.07	0.981	0.420	7.34	0.997	4.87
2,4-DCP	3.08	0.107	3.12	0.970	0.625	9.41	0.955	5.82
2,4,6-TCP	3.69	0.132	3.62	0.964	0.806	10.3	0.969	6.05
PCP	5.01	0.146	3.94	0.982	1.04	13.1	0.955	6.98

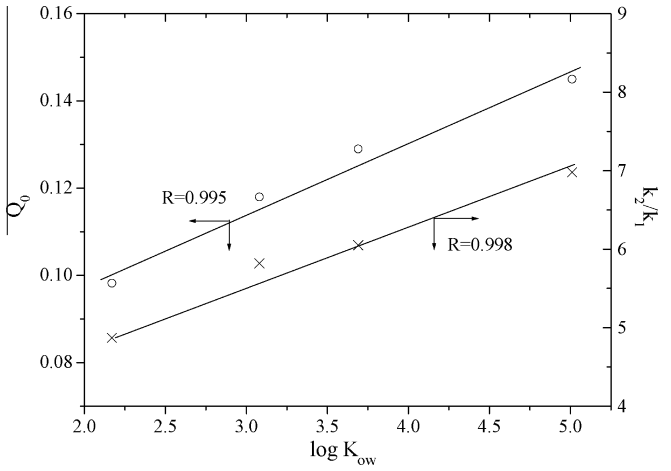

Fig. 3. Relationship of adsorption (Q_0) or enhanced reduction rate (k_2/k_1) with hydrophobicity of CPs ($\log K_{ow}$).

the adsorption of CPs on CTMA-Bent increased dramatically at the low concentrations (<0.5 mM), then reached a near saturation at higher CP concentrations. The saturated adsorption amount of various CPs by CTMA-Bent can be ranked in the increasing order: 2-CP < 2,4-DCP < 2,4,6-TCP < PCP. This implies an increasing adsorption with the increased number of chlorine atoms in the phenol ring of CPs, which corresponds to the increased hydrophobicity as shown by their $\log K_{ow}$ values in Table 1.

The Langmuir equation (Eq. (3)) was employed to quantitatively describe each isotherm. Q_0 is the maximum of adsorption calculated from the Langmuir equation, and used here for comparing the adsorption capacity of various CPs by CMTA-Bent.

$$\frac{1}{Q_e} = \frac{1}{Q_0} + \frac{1}{bQ_0} \cdot \frac{1}{C_e} \tag{3}$$

Fig. 3 shows the relationship between Q_0 and $\log K_{ow}$ for various CPs, and an increasing linear relationship was obtained. This indicates that the adsorption of CPs was determined by their hydrophobicity, and higher hydrophobicity of CPs makes them more readily accessible onto the organically modified bentonite. When the CMTA-Bent was used as the support of NZVI, the hydrophobic CP molecules would tend to gather in the vicinity of solid NZVI/CTMA-Bent composite. As a result, the mass transfer of CPs from aqueous phase to iron surface was facilitated by CTMA-Bent, and the reduction of CPs by NZVI was accelerated (Cho et al., 2005; Li et al., 2011).

In order to verify above mechanisms on the synergetic effect between NZVI and CMTA-Bent, the relative enhancement on reaction rate constants (k_2/k_1) were used to evaluate the enhanced level of

Table 2
Removal efficiencies of CPs in repetitive experiments.

Cycle no.	NZVI				NZVI/CTMA-Bent			
	2-CP (%)	2,4-DCP (%)	2,4,6-TCP (%)	PCP (%)	2-CP (%)	2,4-DCP (%)	2,4,6-TCP (%)	PCP (%)
1	33.5	34.9	38.1	36.4	95.4	96.8	97.8	100
2	25.6	27.7	32.3	29.4	93.6	93.1	95.0	99.4
3	20.2	18.7	21.9	23.8	91.0	92.1	94.6	97.3
4	16.2	17.2	17.0	18.5	88.7	91.4	93.6	96.6

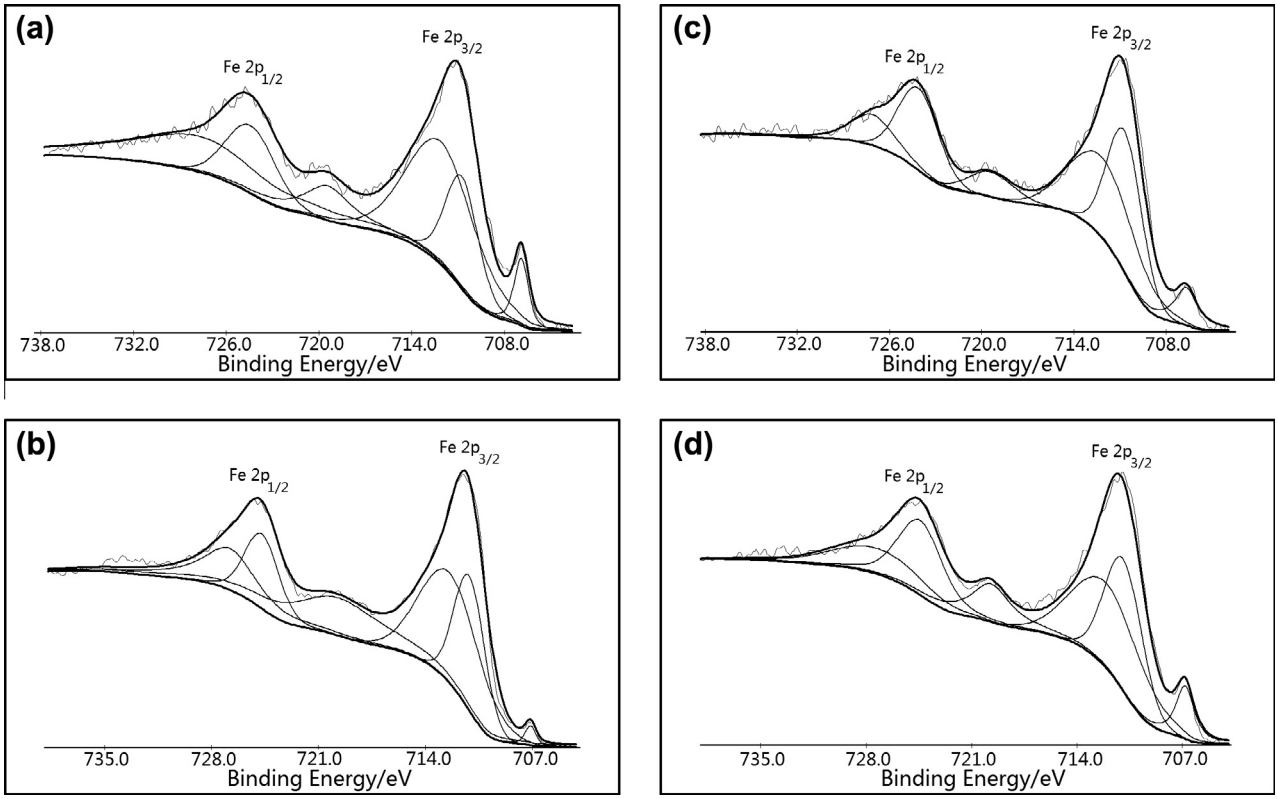

Fig. 4. XPS spectroscopies of Fe 2p from NZVI before (a) and after (b) reaction with PCP, and from NZVI/CTMA-Bent before (c) and after (d) reaction with PCP.

Table 3
Results of decomposed peaks from Fe $2p_{3/2}$.

Fe $2p_{3/2}$	Fe_2O_3		FeOOH		Fe^0	
	Location (eV)	Area (%)	Location (eV)	Area (%)	Location (eV)	Area (%)
NZVI before reaction	710.8	28.4	712.1	63.1	706.9	8.5
NZVI after reaction	711.1	37.4	712.4	60.1	707.1	2.5
NZVI/CTMA-Bent before reaction	710.9	42.6	712.1	46.1	706.7	11.3
NZVI/CTMA-Bent after reaction	710.9	40.3	712.0	48.5	706.8	11.2

CP reduction by NZVI when using CTMA-Bent as the support. Fig. 3 shows that k_2/k_1 increased with the increasing $\log K_{ow}$ of CPs, and a good linear relationship was obtained. This indicates that the higher the hydrophobicity of CPs, the greater the enhancement on reduction rate. Considering the increased adsorption by CTMA-Bent to CPs of high hydrophobicity, a positive relationship is expected between the enhanced reduction rate (k_2/k_1) by NZVI/CTMA-Bent and the adsorption (Q_0) by CTMA-Bent.

Therefore, in the combined reduction system of CPs by NZVI/CTMA-Bent, the adsorption by CTMA-Bent played an essential role on accelerating the reaction. Since the organobentonite has higher adsorption to the more hydrophobic pollutant, the NZVI/CTMA-Bent shows more remarkable enhancement on removing CP with higher hydrophobicity.

3.3. Enhanced stability of NZVI/CTMA-Bent

Respective experiments were conducted to evaluate the repetitive usability of NZVI or NZVI/CTMA-Bent. According to the results illustrated in Table 2, the removal efficiencies of CPs by NZVI decreased by more than 15% after four cycles. However, the efficiencies by NZVI/CTMA-Bent remained high, with a slight decrease. As the reduction proceeding, the ferric oxide and hydroxide will be formed on the iron surface. This will block the reactive sites on the iron surface, which results in lower efficiency on removing CPs. We proposed that the CTMA-Bent, serving as the carrier of NZVI, help decrease the precipitation of oxide and hydroxide on the iron surface.

XPS spectra were employed to investigate the variation of iron species on the surface of NZVI and NZVI/CTMA-Bent before and after reaction with PCP. The observed Fe 2p peaks of NZVI before and after reaction were shown in Fig. 4a and b, respectively, while the Fe 2p peaks of NZVI/CTMA-Bent before and after reaction were shown in Fig. 4c and d, respectively. The $2p_{3/2}$ peaks can be decomposed into three peaks at 706.9 ± 0.2 eV, 710.9 ± 0.2 eV and 712.2 ± 0.2 eV, respectively, which represent the binding energies of Fe^0, Fe_2O_3 and FeOOH, respectively. Similar Fe $2p_{3/2}$ line XPS results were observed in a previous literature (McIntyre and Zetaruk, 1977). As is shown in Table 3, area % of Fe^0 decreased from 8.5% to 2.5% for NZVI after reaction, and area % of Fe_2O_3 increased from 28.4% to 37.4%. This indicated during PCP reduction by NZVI, Fe_2O_3 could be formed and precipitated on the iron surface, which might block the reactivity of NZVI. However, there was no significant change of area % of Fe^0 for NZVI/CTMA-Bent before and after reaction, suggesting a relatively less precipitation of ferric oxide and hydroxide on the solid surface in this treatment. The results are consistent with that observed by XFAS in our investigations on Cr(VI) removal by supported NZVI with the pillared bentonite (Li et al., 2012). The modified bentonite (CTMA-Bent) as the carrier of NZVI could help to transfer some precipitates, and prolong the reactivity of NZVI, so the repetitive usability of NZVI/CTMA-Bent was obtained. Furthermore, the variation of pH during reaction of 2.4-DCP with NZVI and NZVI/CTMA-Bent was monitored. The lower pH in the NZVI/CTMA-Bent treatment (ca. 8.0) than that in the NZVI treatment (ca. 8.4) was observed, possibly due to the buffering effect of aluminol or silanol groups on the bentonite (Powell and Puls, 1997; Oh et al., 2007). The lower pH is also favorable for the enhanced reactivity of NZVI and reduced precipitation of ferric oxide and hydroxide.

4. Conclusions

The NZVI/CTMA-Bent combination has shown enhanced performance on removing CPs in comparison with NZVI alone, indicating a synergetic effect between adsorption by CMTA and reduction by NZVI. The kinetic studies indicated that the enhanced reduction rate by NZVI/CTMA-Bent is positively related to the adsorption of CPs by CTMA-Bent, which showed higher adsorption to the more hydrophobic CP. The repetitive usability of NZVI/CTMA-Bent composite was observed, and related to its improved anti-oxidation according to XPS analysis.

Acknowledgement

This work was supported by the National Natural Science Foundation of China (20977063, 21177088).

Appendix A. Supplementary material

Supplementary data associated with this article can be found, in the online version, at http://dx.doi.org/10.1016/j.chemosphere.2013.01.030.

References

Alessi, D.S., Li, Z., 2001. Synergistic effect of cationic surfactants on perchloroethylene degradation by zero-valent iron. Environ. Sci. Technol. 35, 3713–3717.
Cao, J., Wei, L., Huang, Q., Wang, L., Han, S., 1999. Reducing degradation of azo dye by zero-valent iron in aqueous solution. Chemosphere 38, 565–571.
Cheng, R., Zhou, W., Wang, J., Qi, D., Guo, L., Zhang, W., Qian, Y., 2010. Dechlorination of pentachlorophenol using nanoscale Fe/Ni particles: role of nano-Ni and its size effect. J. Hazard. Mater. 180, 79–85.
Cho, H.-H., Lee, T., Hwang, S.-J., Park, J.-W., 2005. Iron and organo-bentonite for the reduction and sorption of trichloroethylene. Chemosphere 58, 103–108.
Cho, H.-H., Park, J.-W., 2006. Sorption and reduction of tetrachloroethylene with zerovalent iron and amphiphilic molecules. Chemosphere 64, 1047–1052.
Cho, Y., Choi, S., 2010. Degradation of PCE, TCE and 1,1,1-TCA by nanosized FePd bimetallic particles under various experimental conditions. Chemosphere 81, 940–945.
Choe, S., Lee, S.-H., Chang, Y.-Y., Hwang, K.-Y., Khim, J., 2001. Rapid reductive destruction of hazardous organic compounds by nanoscale Fe^0. Chemosphere 42, 367–372.
Dries, J., Bastiaens, L., Springael, D., Agathos, S.N., Diels, L., 2004. Competition for sorption and degradation of chlorinated ethenes in batch zero-valent iron systems. Environ. Sci. Technol. 38, 2879–2884.
Elliott, D.W., Zhang, W.X., 2001. Field assessment of nanoscale bimetallic particles for groundwater treatment. Environ. Sci. Technol. 35, 4922–4926.
Feng, J., Lim, T., 2005. Pathways and kinetics of carbon tetrachloride and chloroform reductions by nano-scale Fe and Fe/Ni particles: comparison with commercial micro-scale Fe and Zn. Chemosphere 59, 1267–1277.
Gillham, R.W., O'Hannesin, S.F., 1994. Enhanced degradation of halogenated aliphatics by zerovalent iron. Ground Water 32, 958–967.
Habekost, A., Aristov, N., 2012. Heterogeneous reductive dehalogenation of PCB contaminated transformer oil and brominated diphenyl ethers with zero valent iron. Chemosphere 88, 1283–1286.
Kim, Y., Carraway, E.R., 2000. Dechlorination of pentachlorophenol by zero valent iron and modified zero valent irons. Environ. Sci. Technol. 34, 2014–2017.

Li, A., Tai, C., Zhao, Z., Wang, Y., Zhang, Q., Jiang, G., Hu, J., 2007. Debromination of decabrominated diphenyl ether by resin-bound iron nanoparticles. Environ. Sci. Technol. 41, 6841–6846.
Li, J., Li, Y., Dong, H., 2008. Controlled release of herbicide acetochlor from clay/carboxylmethylcellulose gel formulations. J. Agric. Food Chem. 56, 1336–1342.
Li, J., Li, Y., Meng, Q., 2010. Removal of nitrate by zero-valent iron and pillared bentonite. J. Hazard. Mater. 174, 188–193.
Li, Y., Li, J., Zhang, Y., 2012. Mechanism insights into enhanced Cr(VI) removal using nanoscale zerovalent iron supported on the pillared bentonite by macroscopic and spectroscopic studies. J. Hazard. Mater. 227–228, 211–218.
Li, Y., Zhang, Y., Li, J., Zheng, X., 2011. Enhanced removal of pentachlorophenol by a novel composite: nanoscale zero valent iron immobilized on organobentonite. Environ. Pollut. 159, 3744–3749.
Li, Z., Jones, H.K., Bowman, R.S., 1999. Enhanced reduction of chromate and PCE by pelletized surfactant-modified zeolite/zerovalent iron. Environ. Sci. Technol. 33, 4326–4330.
Liu, Y.Q., Choi, H., Dionysiou, D., Lowry, G.V., 2005. Trichloroethene hydrodechlorination in water by highly disordered monometallic nanoiron. Chem. Mater. 17, 5315–5322.
Loraine, G.A., 2001. Effects of alcohols, anionic and nonionic surfactants on the reduction of PCE and TCE by zero-valent iron. Water Res. 35, 1453–1460.
Ma, J., Zhu, L., 2007. Removal of phenols from water accompanied with synthesis of organobentonite in one-step process. Chemosphere 68, 1883–1888.
McIntyre, N.S., Zetaruk, D.G., 1977. X-ray photoelectron spectroscopic studies of iron oxides. Anal. Chem. 49, 1521–1529.
Oh, Y.J., Song, H., Shin, W.S., Choi, S.J., Kim, Y.H., 2007. Effect of amorphous silica and silica sand on removal of chromium(VI) by zero-valent iron. Chemosphere 66, 858–865.
Phenrat, T., Saleh, N., Sirk, K., Tilton, R.D., Lowry, G.V., 2007. Aggregation and sedimentation of aqueous nanoscale zerovalent iron dispersions. Environ. Sci. Technol. 41, 284–290.
Ponder, S.M., Darab, J.G., Mallourk, T.E., 2000. Remediation of Cr(VI) and Pb(II) aqueous solutions using supported, nanoscale zero-valent iron. Environ. Sci. Technol. 34, 2564–2569.
Powell, R.M., Puls, R.W., 1997. Proton generation by dissolution of intrinsic or augmented aluminosilicate minerals for in situ contaminant remediation by zero-valence-state iron. Environ. Sci. Technol. 31, 2244–2251.
Saad, R., Thiboutot, S., Ampleman, G., Wang, D., Hawari, J., 2010. Degradation of trinitroglycerin (TNG) using zero-valent iron nanoparticles/nanosilica SBA-15 composite (ZVINs/SBA-15). Chemosphere 81, 853–858.
Sayles, G.D., You, G., Wang, M., Kupferle, M.J., 1997. DDT, DDD, and DDE dechlorination by zero-valent iron. Environ. Sci. Technol. 31, 3448–3454.
Wang, C., Zhang, W., 1997. Synthesizing nanoscale iron particles for rapid and complete dechlorination of TCE and PCBs. Environ. Sci. Technol. 31, 2154–2156.
Wang, H., Fu, Y., Wang, C., Guo, Q., 2008a. Theoretical study of homolytic C–Cl bond dissociation enthalpies of environmental pollutants. Acta Chim. Sinica 66, 362–370 (Published in Chinese).
Wang, X., Chen, C., Liu, H., Ma, J., 2008b. Preparation and characterization of PAA/PVDF membrane-immobilized Pd/Fe nanoparticles for dechlorination of trichloroacetic acid. Water Res. 42, 4656–4664.
Wei, J., Xu, X., Liu, Y., Wang, D., 2006. Catalytic hydrodechlorination of 2,4-dichlorophenol over nanoscale Pd/Fe: reaction pathway and some experimental parameters. Water Res. 40, 348–354.
Wu, L., Ritchie, S.M.C., 2006. Removal of trichloroethylene from water by cellulose acetate supported bimetallic Ni/Fe nanoparticles. Chemosphere 63, 285–292.
Yoon, I.-H., Kim, K.-W., Bang, S., Kim, M.G., 2011. Reduction and adsorption mechanisms of selenate by zero-valent iron and related iron corrosion. Appl. Catal. B: Environ. 104, 185–192.
Zhang, P., Tao, X., Li, Z., Bowman, R.S., 2002. Enhanced perchloroethylene reduction in column systems using surfactant-modified zeolite/zero-valent iron pellets. Environ. Sci. Technol. 36, 3597–3603.
Zheng, T., Zhan, J., He, J., Day, C., Lu, Y., McPerson, G.L., Piringer, G., John, V.T., 2008. Reactivity characteristics of nanoscale zerovalent iron–silica composites for trichloroethylene remediation. Environ. Sci. Technol. 42, 4494–4499.
Zhu, L., Li, Y., Zhang, J., 1997. Sorption of organobentonites to some organic pollutants in water. Environ. Sci. Technol. 31, 1407–1410.